

of the experimental results quite well. Starting point of the theory is Bohr's collective Hamiltonian. The six kinetic-energy functions and the potential-energy function which enter into the Hamiltonian are derived from the pairing-plus-quadrupole model of residual interactions. The Hamiltonian is then diagonalized exactly by a numerical method. The solid curve in Fig. 6 is drawn through the predictions of this theory. The higher experimental points correspond to the theoretical prediction for the sign of the interference term. Within the experimental error, the agreement between experiment and theory is quite remarkable, especially as to the sign of Q_2^+ . Measurements on the isotopes of Os which are in progress⁸ confirm the predicted change in the sign of Q_2^+ in this region.

⁸ R. J. Pryor, J. X. Saladin, J. R. Kerns, and S. Lane, *Bull. Am. Phys. Soc.* **14**, 123 (1969).

The dashed line is drawn through values obtained from the symmetric-rotor-model relation

$$(M_{22}/M_{12})^2 = 10/7$$

using experimental values for M_{12} .

ACKNOWLEDGMENT

It is a pleasure to acknowledge stimulating discussions and correspondence with Professor K. Alder, Professor M. Baranger, Dr. K. Kumar, and Dr. H. Pauli. We are very much indebted to J. R. Kerns and Dr. P. Crowley for extensive help in accumulating and analyzing the data. One of us (J.X.S.) is very grateful for the hospitality of the Physics Department of the University of Basel where part of this paper was written.

Prompt K X Rays as a Function of Fragment Mass and Total Kinetic Energy in the Thermal Fission of U^{235} †*

E. M. BOHN,† B. W. WEHRING, AND M. E. WYMAN

Nuclear Engineering Program, University of Illinois, Urbana, Illinois 61801

(Received 11 August 1969)

In order to obtain information about the deexcitation of fission fragments and the division of nuclear charge in fission for the case of thermal-neutron fission of U^{235} , a measurement of the prompt K x rays (0 to ~ 1 nsec after fission) was performed. A thin foil of uranium was caused to fission by a beam of neutrons from a beam port of a nuclear reactor. The fission fragments were detected by silicon surface-barrier detectors, and the x rays, by a NaI(Tl) scintillator. A three-parameter analyzer recorded the energies of the two fragments and the energy of the x ray emitted in coincidence with the fragments. The x-ray energies were sorted "off line" according to fragment mass or total kinetic energy in order to obtain x-ray spectra for different mass groups and different energy groups. From these spectra, x-ray yields were found as a function of fragment mass and as a function of total kinetic energy of the fragments. The results are compared, where possible, with those obtained in other laboratories for the thermal-neutron fission of U^{235} and with results for the spontaneous fission of Cf^{252} . Differences and similarities are noted. The most probable charge versus mass was also estimated from the spectra, and these results are in agreement with radiochemical analysis.

I. INTRODUCTION

RECENTLY, a great deal of interest has developed in the study of K x rays emitted by excited fission fragments. The interest has been stimulated by the fact that such studies lead to information about the charge division in fission. Also of importance is the information about fragment deexcitation processes found by the investigations.

Many studies of the K x rays coincident with the

spontaneous fission of Cf^{252} have been performed.¹⁻⁶ Glendenin and Griffin¹ reported that a total of $0.55 \pm 0.05K$ x rays per fission were emitted between 0 and ~ 0.3 μ sec after fission, and that the times of emission were characteristic of the internal conversion process. Further studies^{2-4,6} showed that for various time intervals after fission, K x-ray yields per fragment depend on fragment mass. More recently, high-

¹ L. E. Glendenin and H. C. Griffin, *Phys. Letters* **15**, 153 (1965).

² L. E. Glendenin and J. P. Unik, *Phys. Rev.* **140**, B1301 (1965).

³ S. S. Kapoor, H. R. Bowman, and S. G. Thompson, *Phys. Rev.* **140**, B1310 (1965).

⁴ R. A. Atneosen, T. D. Thomas, W. M. Gibson, and M. L. Perlman, *Phys. Rev.* **148**, 1206 (1966).

⁵ R. L. Watson, H. R. Bowman, and S. G. Thompson, *Phys. Rev.* **162**, 1169 (1967).

⁶ A. B. Long, B. W. Wehring, and M. E. Wyman, *Phys. Rev.* **188**, 1948 (1969).

† The work reported in this article was supported by the National Science Foundation.

* The material in this article is based upon a dissertation by one of the authors (EMB) submitted in partial fulfillment of the requirements for the doctoral degree at the University of Illinois.

‡ Present address: Reactor Physics Division, Argonne National Laboratory, Argonne, Ill.

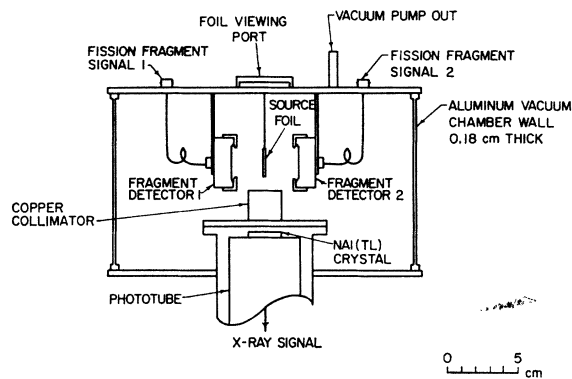


FIG. 1. Vacuum chamber containing source foil, x-ray detector and fragment detectors.

resolution measurements⁵ have shown a dependence for the K x-ray yields per fragment on fragment atomic number.

Results of measurements on the K x rays coincident with thermal-neutron fission of U^{235} also are numerous.⁷⁻¹³ Bridwell, Wyman, and Wehring⁹ found that $0.60 \pm 0.06K$ x rays per fission¹⁴ were emitted between 0 and $\sim 0.3 \mu\text{sec}$ after fission, and that the times of emission were characteristic of the internal conversion process, as was found for Cf^{252} . A dependence of the K x-ray yields per fragment on the fragment mass¹¹⁻¹³ and on the fragment atomic number^{10,13} was also found for thermal-neutron fission of U^{235} .

The present work concerns the measurement of K x rays as a function of fragment mass and total kinetic energy in the thermal-neutron fission of U^{235} . In order to identify the masses of the fragments emitting the x rays, it was necessary to perform a three-parameter experiment in which the energies of the two fission fragments were recorded along with the energy of the x rays emitted in coincidence with the fragments. The detectors and detector geometry were similar to those used by Glendenin,² and therefore direct comparison can be made between the results for U^{235} and the results for Cf^{252} . The final analysis of the three-parameter data is reported in this paper. Some of these results were previously reported in preliminary form.¹¹

⁷ V. V. Sklyarevskii, E. P. Stepanov, and B. A. Medvedev, Zh. Eksperim. i Teor. Fiz. **36**, 326 (1959) [English transl.: Soviet Phys.—JETP **9**, 225 (1959)].

⁸ H. Hohman, Z. Physik **172**, 143 (1963).

⁹ L. Bridwell, M. E. Wyman, and B. E. Wehring, Phys. Rev. **145**, 963 (1966).

¹⁰ B. W. Wehring and M. E. Wyman, Phys. Rev. **157**, 1083 (1967).

¹¹ E. M. Bohn, B. W. Wehring, and M. E. Wyman, Appl. Phys. Letters **12**, 199 (1968).

¹² S. S. Kapoor, V. S. Ramamurthy, and R. Zaghoul, Phys. Rev. **177**, 1776 (1969).

¹³ L. E. Glendenin (private communication).

¹⁴ The agreement between many of the earlier results for the number of K x rays per fission may have appeared to be poor, but when the detection geometries and emission times are taken into account most of the results are consistent with the yields given in Ref. 9.

II. EXPERIMENT

A. Detection System

The system which was developed for the experiment is shown in Fig. 1. The source foil was an uranium oxide deposit enriched to 93% U^{235} , covering a circular area of 1.1 cm^2 and approximately $70 \mu\text{g}/\text{cm}^2$ thick. It was prepared by vacuum evaporation of UO_2 onto a nickel backing $90 \mu\text{g}/\text{cm}^2$ thick. The deposit was thick enough to give a reasonable fission rate in available neutron fluxes, and thin enough to preserve adequate mass resolution.

The fragment detectors were silicon surface-barrier detectors with sensitive areas of 400 mm^2 . Each detector was located 2.4 cm from the source foil. The sensitive area of each fragment detector was reduced to the center 254 mm^2 by the use of aluminum apertures to eliminate edge effects in the fragment spectrum.

The x-ray detector was a 1-mm-thick NaI(Tl) scintillator mounted on an RCA 6342A phototube, covered by a 0.13-mm-thick Be window and presenting an active circular area of 3.37 cm^2 at 5 cm from the source foil. The detector was restricted by a cylindrical copper collimator to view the first centimeter of fragment path. The results of timing measurements of the K x rays from U^{235} fission⁹ indicated that about half of the x rays are emitted within 1 nsec after fission. Using an average velocity of $10^9 \text{ cm}/\text{sec}$ for the fragments, one sees that the first centimeter of fragment path corresponds to the time of about 1 nsec after fission.

The source foil and fragment detectors were placed in a cylindrical aluminum vacuum chamber (maintained at 10^{-2} Torr) having a 0.18-cm-thick wall. The x-ray detector was located outside the vacuum and viewed the source foil through a 0.025-mm Mylar window. The chamber was located at the tangential beam port of the University of Illinois TRIGA nuclear reactor. A narrow beam of neutrons [spread of 1 cm full width at half-maximum (FWHM) at 10 cm from the collimator face] was allowed to enter the chamber through the chamber wall, pass through the center of the chamber impinging only on the source foil, and exit through the chamber

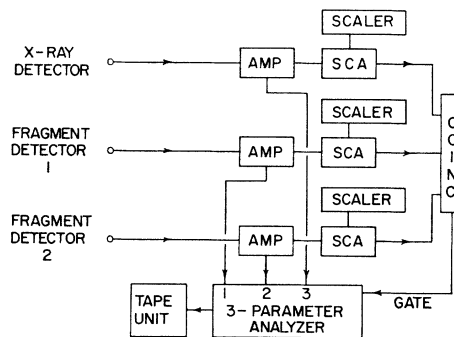


FIG. 2. Data recording system.

wall. The thin aluminum chamber wall held neutron and γ scattering from the beam to a minimum.

The data recording system is shown in Fig. 2. The three detector signals were sent to preamplifiers, amplifiers, and a coincidence unit. The coincidence resolving time (2τ) was $0.4 \mu\text{sec}$. Coincidence sets of pulse heights were analyzed and stored in a buffer memory which was dumped onto magnetic tape. Magnetic tapes were analyzed "off line" on an IBM 7094 computer.

B. Mass Analysis

The following is a brief discussion of the mass analysis used. This topic will be discussed more fully elsewhere.¹⁵ The preneutron-emission masses m_1^* and m_2^* were calculated from the fragment kinetic energies by using the following relationships:

$$\begin{aligned} m_1^* &= A E_2 / (Q E_1 + E_2), \\ m_2^* &= A - m_1^*, \end{aligned} \quad (1)$$

$$Q = (1 + \nu_1/m_1)(1 + \nu_2/m_2)^{-1},$$

where A is the mass of the fissioning nucleus, E_i is the energy of fragment i measured by detector i , ν_i is the average number of neutrons emitted by fragments of mass m_i^* , and m_i is the mass of fragment i after neutron emission ($m_i^* = m_i + \nu_i$). The fragment energies at the detectors were related to the recorded pulse heights by

$$E_i = (A_i + B_i m_i) X_i + (C_i + D_i m_i), \quad (2)$$

where A_i , B_i , C_i , and D_i are constants characterized by detector i and determined as described by Schmitt *et al.*,¹⁶ and X_i are the recorded pulse heights. Because Eq. (2) contains the unknown final masses m_i , an iteration process was developed to solve for m_1^* and m_2^* given pulse heights X_1 and X_2 . For each iteration, the values of ν_i were taken from experimental data of Milton and Fraser¹⁷ according to the values of m_i^* obtained for the previous iteration. A convergence criterion of 0.1 amu was used. After convergence, the preneutron-emission energies were found from

$$E_i^* = (m_i^*/m_i) E_i. \quad (3)$$

The mass resolution of this type of experiment (i.e., event-by-event calculation of mass) is of the order of 4 amu. However, it is necessary to establish the mass resolution as accurately as possible in order to correct for mass dispersion effects in the x-ray yields and the most probable charge as a function of mass. The mass

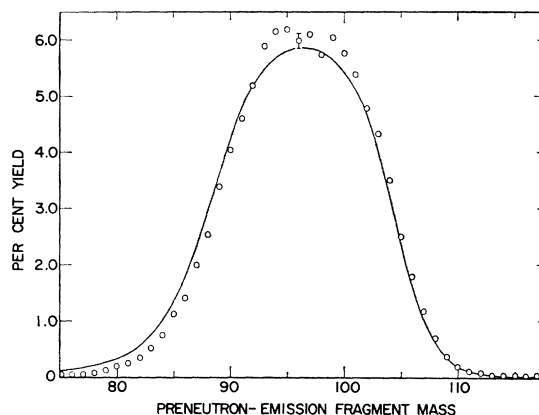


FIG. 3. Preneutron-emission mass distribution from thermal-neutron fission of U^{235} . The points are experimental values obtained in this experiment. The line is the result of folding (FWHM = 5.0 amu) an undispersed mass distribution estimated by unfolding the time-of-flight results of Milton and Fraser (Ref. 18).

resolution as a function of m_1^* was taken to be

$$\begin{aligned} \sigma^2(m_1^*) &= (m_1^* m_2^* / A)^2 [\sigma^2(E_1) / E_1^2 + \sigma^2(E_2) / E_2^2 \\ &\quad + \sigma^2(\nu_1) / m_1^2 + \sigma^2(\nu_2) / m_2^2], \end{aligned} \quad (4)$$

where $\sigma^2(E_i)$ is the variance of E_i , and $\sigma^2(\nu_i)$ is the variance of the number of neutrons emitted by fragments of specified mass. The variance of E_i is given by

$$\sigma^2(E_i) = \frac{4}{3} \nu_i E_i E_n / m_i + \sigma_D^2 + \sigma_S^2 + \sigma_C^2 + \sigma_c^2, \quad (5)$$

where E_n is the average neutron energy in the fragment center-of-mass, σ_D^2 is the variance due to fragment detector resolution (FWHM = 1.5 MeV), σ_S^2 is the variance due to the thickness of the source deposit (and Ni backing for one of the fragments), σ_C^2 is the variance due to analyzer grouping, and σ_c^2 is a variable variance to allow for additional energy variance from unaccountable sources (e.g., fragment detector radiation damage). Experimental values of ν_i , E_n ¹⁷ and E_i ¹⁸ as a function of m^* were used for the calculations. The value of $\sigma^2(\nu_i)$ was taken from Terrell.¹⁹

Equation (4) gives the mass resolution in the experiment when the proper value of σ_c^2 is determined. In order to find σ_c^2 , time-of-flight mass-yield data of Milton and Fraser¹⁸ were unfolded to obtain an estimate of the undispersed mass-yield distribution for thermal fission of U^{235} . The undispersed mass yield distribution was then folded with a Gaussian response function having the variance given by Eq. (4). Folded distributions were calculated for many values of σ_c^2 .

An experimental mass distribution was determined by performing a double-fragment measurement in which

¹⁵ E. M. Bohn, A. B. Long, R. D. Rollins, B. W. Wehring, and M. E. Wyman (unpublished).

¹⁶ H. W. Schmitt, W. E. Kiker, and C. W. Williams, Phys. Rev. **137**, B837 (1965).

¹⁷ J. C. D. Milton and J. S. Fraser, Canadian Atomic Energy Commission Report No. AECL SM-60/45, 1964 (unpublished).

¹⁸ J. C. D. Milton and J. S. Fraser, Can. J. Phys. **40**, 1626 (1962).

¹⁹ J. Terrell, Phys. Rev. **127**, 880 (1962).

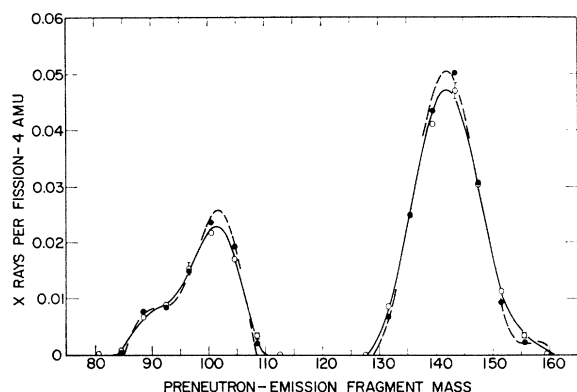


FIG. 4. K x-ray yields per fission for times of 0 to ~ 1 nsec after thermal-neutron fission of U^{235} . The open points are the measured values uncorrected for mass dispersion. The solid lines are the result of least-squares fitting 8th-order polynomials to the yields. The dashed lines are the result of unfolding (FWHM = 5 amu) the solid lines. The solid points are the corrected yields.

only the energies of the two fragments were recorded. The result of such a measurement is shown in Fig. 3. The value of σ_C^2 of the folded distribution (also shown in Fig. 3) which best matched the results of the experiment was then used in Eq. (4). It was determined that the mass resolution obtained for the three-parameter experiment was 5.0 amu FWHM.

As pointed out by Schmitt,²⁰ the time-of-flight data¹⁸ was taken without antiscattering baffles on the flight tubes. The resulting effect was to disperse and shift down in mass the mass distribution computed from the time-of-flight measurements. This would account for the small differences between the measured and calculated mass distribution shown in Fig. 3.

C. X-Ray Spectra

The x-ray detector was calibrated by recording spectra for two K x-ray emitting isotopes, Ag^{109} and Rb^{85} . The average energies of these spectra were calculated from the energy of the $K\alpha_1$, $K\alpha_2$, $K\beta_1$, and $K\beta_2$ lines using relative intensities from Wapstra.²¹ Spectrum shifts due to gain change or high-voltage changes in the x-ray channel were measured by recording and comparing Ag^{109} and Rb^{85} spectra before and after a data run. For the small shifts that were present, averaged channel numbers computed from the two sets of calibrating spectra were used for calibration.

At a reactor power of 250 kW, the gross triple-coincidence count rate was 0.85/sec. Three data runs lasting approximately eight hours each were combined to obtain a total of 40 000 triple coincidence events. The background was measured by covering the x-ray

detector with a copper disk 0.7 mm thick. This thickness of copper absorbed most of the x rays up to 45 keV. Background data were recorded for a period of three hours and normalized to the total gross spectrum.

Using the preneutron-emission masses calculated from the fission fragment pulse heights accompanying each x-ray pulse height, the computer sorted the gross and background data into mass groups 4 amu wide. The number of x rays as a function of x-ray energy for different mass groups was thus obtained. In addition, x-ray spectra as a function of total fragment kinetic energy were obtained for total kinetic energy intervals 5 MeV wide. The total fragment energy was computed by summing the two initial fragment energies calculated during the mass computation.

III. RESULTS AND DISCUSSION

A. X-Ray Yields as Function of Fragment Mass

The net x-ray spectrum (background subtracted) for each mass group was summed over x-ray energy to obtain x-ray yields as a function of mass. These yields were corrected for the efficiency of the NaI(Tl) detector and for the escape probability of the iodine K x ray from the crystal. The solid angle for x-ray detection was computed assuming that the x-rays were emitted at the source foil. The aluminum ring of the source holder blocked a small portion of the x rays from reaching the detector and was included as a correction to the solid angle. The results for each mass group were then divided by the total number of fissions detected to obtain the x-ray yield per fission. The number of fissions detected was determined from the count rate of one of the fragment detectors times the conditional probability of detecting both fragments.

The x-ray yield per fission for each 4-amu mass interval plotted at the median mass is shown in Fig. 4. The uncertainties indicated are standard errors due to uncertainties in the gross and background x-ray spectra. The solid lines shown in Fig. 4 are the result of least-squares fitting two 8th-order polynomials to points chosen at 1-amu intervals in such a way as to preserve x-ray yields in each 4-amu interval. The dashed lines are the result of unfolding the solid lines with a Gaussian response function having a FWHM equal to 5.0 amu. The unfolding method used was the one suggested by Grissom *et al.*²² The solid lines and dashed lines were then used to correct for mass dispersion the measured x-ray yields per fission (open points in Fig. 4) to give the corrected yields per fission (solid points in Fig. 4).

Summing the yields gave 0.07 ± 0.01 x rays per fission for the light fragments, and 0.17 ± 0.02 x rays per fission for the heavy fragments. An uncertainty of 12% in the

²⁰ H. W. Schmitt, J. H. Neiler, and F. J. Walter, *Phy. Rev.* **141**, 1146 (1966).

²¹ A. H. Wapstra, G. J. Nijgh, and R. Van Lieshout, *Nuclear Spectroscopy Tables* (North-Holland Publishing Co., Amsterdam, 1959).

²² J. T. Grissom, D. R. Koehler, and B. G. Gibbs, *Nucl. Instr. Methods* **45**, 190 (1966).

determination of the x-ray solid angle has been included. These results agree with those of Kapoor¹² and are consistent with those of Bridwell.⁹ It was also found that the measured x-ray yields for mass intervals 83–86 and 126–129 could be attributed entirely (within experimental error) to mass intervals 87–90 and 130–133, respectively.

The measured x-ray yields per fission divided by the measured mass yield (fragments per 4 amu per fission found from the experimental results shown in Fig. 3) gave the x-ray yields per fragment shown as open points in Fig. 5. The corrected x-ray yields per fission divided by a corrected mass yield gave the x-ray yields per fragment shown as solid points in Fig. 5. The corrected mass yield used was found by correcting the experimental results shown in Fig. 3.

The x-ray yield per fragment is replotted in Fig. 6 for postneutron-emission mass found using neutron emission data of Milton and Fraser.¹⁷ The results for spontaneously fissioning Cf^{252} obtained by Glendenin² along with the results of Kapoor¹² for thermal-neutron fission of U^{235} are also shown in Fig. 6. The results selected from Kapoor's work are the yields associated with short times after fission (termed partly shielded view in Ref. 12). These results should correspond to the 1-nsec yields of the present investigation.

Within experimental error, our results agree with those of Kapoor with the possible exception of the peak at mass 87. As expected, the light fragment x-ray yields per fragment rise from a minimum near mass 82, corresponding to the closed neutron shell $N=50$, and then increase with increasing mass. The heavy fragment x-ray yields exhibit a minimum near mass 128, corresponding to fragments near the closed proton shell $Z=50$. The x-ray yield per fragment then increase with increasing mass as was found for the light fragments.

This general behavior is also shown by the x-ray

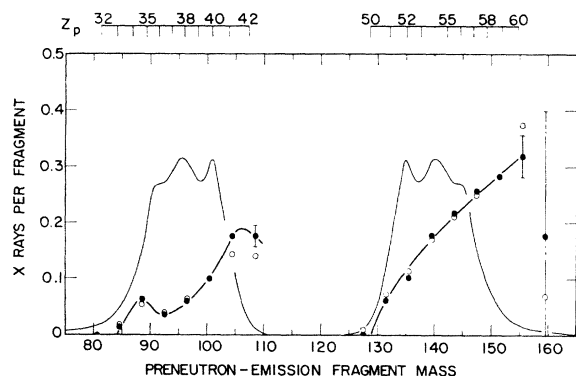


FIG. 5. K x-ray yields per fragment for times of 0 to ~ 1 nsec after thermal-neutron fission of U^{235} . The open points are results uncorrected for mass dispersion and the solid points are results corrected for mass dispersion. Also shown is the undispersed mass distribution estimated by unfolding the time-of-flight data of Milton and Fraser (Ref. 18).

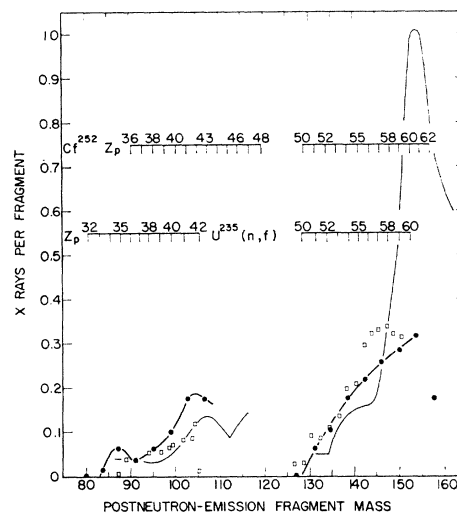


FIG. 6. Comparison between K x-ray yields per fragment for times of 0 to ~ 1 nsec after thermal-neutron fission of U^{235} and spontaneous fission of Cf^{252} . The solid points are the solid points given in Fig. 5 replotted versus postneutron-emission mass. The open squares are the data obtained by Kapoor *et al.* for U^{235} (Ref. 12) and the light solid line represents the data obtained for Cf^{252} (Ref. 2).

yields from the fission of Cf^{252} and, in fact, the values of the yields are the same within experimental error except for fragments heavier than mass 145. For these heaviest heavy fragments, the x-ray yields per fragment appear to be different for the two cases. For example, fragments with postneutron-emission mass 153 ($Z=60$) on the average emit about $1K$ x ray per fragment for Cf^{252} and apparently only about $0.3K$ x rays per fragment for U^{235} . Kapoor¹² suggests that the absence of the striking increase in the x-ray yield for masses greater than 144 for the case of thermal-neutron fission of U^{235} is due to the corresponding complementary (light) fragments being spherical.

B. X-Ray Yields as Function of Total Kinetic Energy

The net x-ray spectrum (background subtracted) for each total-kinetic-energy group was summed over x-ray energy for the light and for the heavy fragments in order to obtain x-ray yields as a function of total kinetic energy. The results were corrected in the same manner as before for detector efficiency, escape peak, solid angle, and fission rate to give the x-ray yield per 5 MeV per fission. These yields were then divided by the experimentally determined total-kinetic-energy yield (shown in the upper graph of Fig. 7) to give the x-ray yield per fragment as a function of total kinetic energy (shown in the lower graph of Fig. 7). The result for the light fragment yield is relatively constant, while the heavy fragment yield shows a striking increase for total kinetic energy less than 160 MeV.

Since total kinetic energy and mass division are

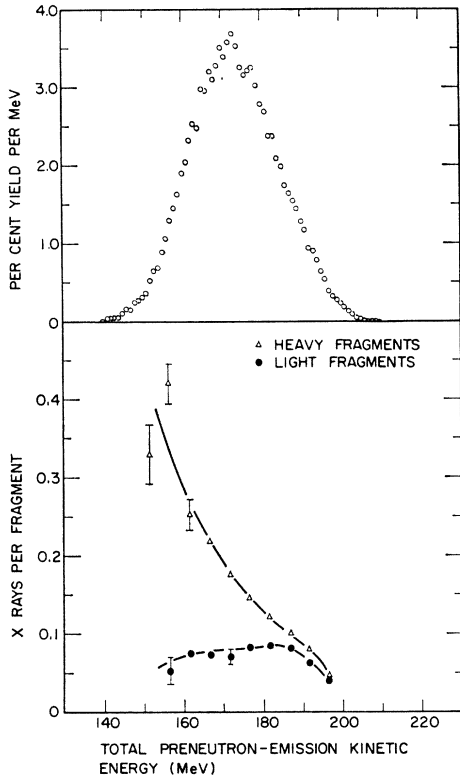


FIG. 7. Total-kinetic-energy yield for thermal-neutron fission of U^{235} measured in this experiment (upper graph) and K x-ray yields per fragment for times of 0 to ~ 1 nsec after thermal-neutron fission of U^{235} (lower graph).

correlated (high kinetic energy with more symmetric fission and low kinetic energy with more asymmetric fission), the dependence of the x-ray yield per fragment on mass should show up as a dependence on total

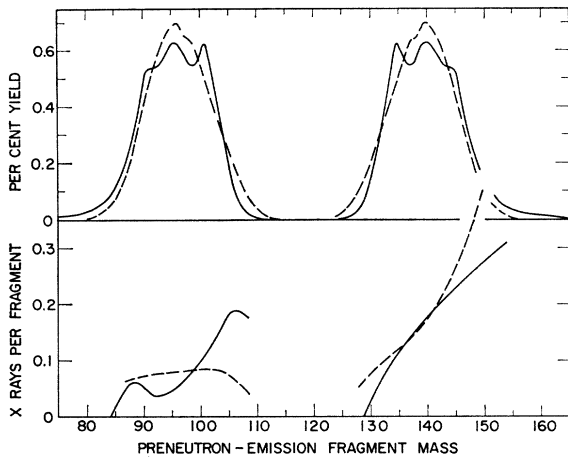


FIG. 8. Results shown in Fig. 7 placed on top of results shown in Fig. 5. The solid lines are the mass yield (upper graph) and the x-ray yields per fragment (lower graph) versus mass. The dashed lines are the total-kinetic-energy yield (upper graph) and the x-ray yields per fragment (lower graph) versus total kinetic energy.

kinetic energy. Any true correlation with kinetic energy is expected to be small since most of the x rays are believed to be due to internal conversion of transitions from low-lying energy levels. The x-ray data sorted as a function of total kinetic energy, therefore, should exhibit the general trends of the x-ray data sorted according to mass. However, no structure would be expected since the total-kinetic-energy distribution for any fragment mass is broad.

In order to compare the x-ray yield as a function of fragment mass with the x-ray yields as a function of total kinetic energy, the graphs in Fig. 7 were simply placed over the graphs in Fig. 5. This is shown in Fig. 8. The solid lines are the fragment mass yield (upper

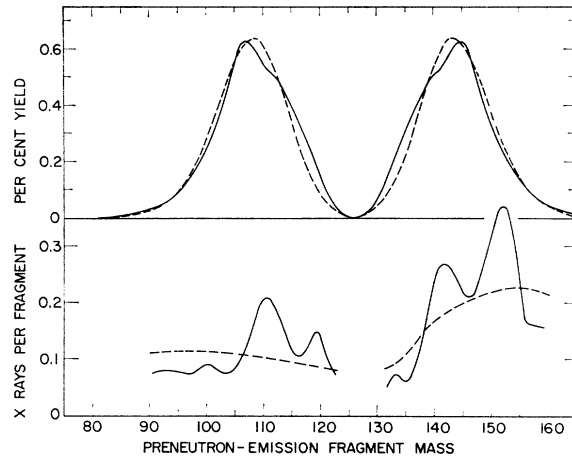


FIG. 9. Similar comparison as shown in Fig. 8 made for K x rays emitted between 1 and 56 nsec after spontaneous fission of Cf^{252} (Ref. 6). The solid lines are the mass yield (upper graph) and the x-ray yields per fragment (lower graph) versus mass. The dashed lines are the total-kinetic-energy yield (upper graph) and the x-ray yields per fragment (lower graph) versus total kinetic energy.

graph) and the x-ray yields per fragment (lower graph) versus mass. The dashed lines are the total-kinetic-energy yield (upper graph) and the x-ray yields per fragment (lower graph) versus total kinetic energy. The dashed lines were positioned so that the total-kinetic-energy yield fell on top of the corresponding fragment mass yield. For the light fragments, total kinetic energy increases with increasing mass, and for the heavy fragments, total kinetic energy decreases with increasing mass. This type of comparison also was made for the x-ray yields measured by Long⁶ for times of 1-56 nsec after the fission of Cf^{252} , and is shown in Fig. 9.

The results of such comparisons seem to bear out the argument that any dependence on kinetic energy can be explained by the dependence on fragment mass and the broad correlation between the two except for the heaviest heavy fragments from the fission of U^{235} . Here, the x-ray yield per fission appears to depend on total

kinetic energy more strongly than on fragment mass. This would appear to be a contradiction, since an x-ray yield only dependent on mass would appear to be smeared out when plotted against total kinetic energy. One possible conclusion is that the x-ray yield is dependent on the total fragment kinetic energy. Another conclusion is that some uncertainty was not taken into account in the determination of the mass of the heaviest of the heavy fragments. Further work will be required to determine which conclusion is valid.

C. Most Probable Charge as Function of Mass

The x-ray spectrum for each 4-amu mass interval was analyzed for the most probable charge Z_p associated with that mass interval. The most probable charge was taken as the Z number corresponding to the energy of the maximum of the x-ray peak. The average K x-ray energy as a function of Z given by Wapstra *et al.*²¹ was used for the assignment.

The Z_p for each mass interval plotted at the average mass for the mass interval is given in Fig. 10. The average mass was computed using as weighting the measured x-ray yield per fission as a function of mass. The solid points are the results for the light fragments and the open points for the heavy fragments. The estimated uncertainty in Z_p is $\pm 0.5Z$ units, and the estimated uncertainty in the average mass is ± 0.5 amu. Also shown in Fig. 10 as a solid line is the most probable charge predicted by Wahl²³ from radiochemical studies. The agreement between the x-ray results and the radiochemical results is quite good except for masses less than 90 and greater than 145. In this region, however, the x-ray results for Z_p for the light and heavy fragments are not consistent with each other.

It is reasonable to believe that there are regions of masses for which there is selective x-ray emission from some isotopes. These fluctuations, however, are averaged by the resolution of the x-ray detector (FWHM = $6Z$) and the resolution of mass system (FWHM = 5 amu). If the Z_p for any mass interval is biased by selective emission, the average mass assigned to that mass interval is also biased, since the weighting for the average mass was calculated from the x-ray yields. This effect tends to put the measured Z_p value back on the correct Z_p curve. The x-ray results, then, should give a good indication of Z_p .

We are not able to explain the difference between the Z_p found from the light-fragment x-ray data and the Z_p from the heavy-fragment x-ray data for masses less than 90 and greater than 145. It should be noted, however, that a displacement of the average mass off the Z_p curve in the directions indicated in Fig. 10 is consistent with an increase in the x-ray yield around mass

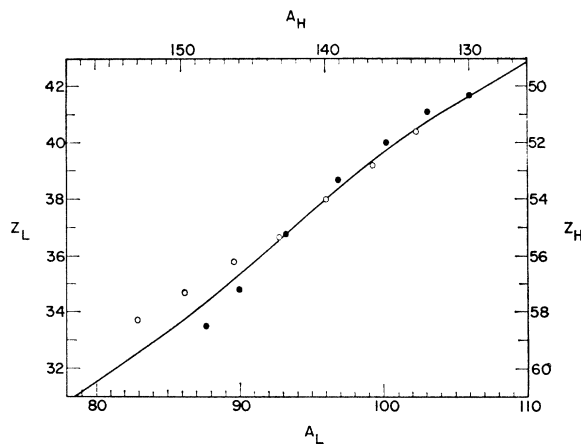


FIG. 10. Most probable charge Z_p versus preneutron-emission mass. The closed points are the results found from the light-fragment x-ray data and the open points are the results found from the heavy-fragment x-ray data. The solid line is the radiochemical result. (Ref. 23).

87 and a decrease in the x-ray yield for masses heavier than 145. If the points in Fig. 10 were moved back to the Z_p curve, the peak at mass 87 (Fig. 6) would become less distinct in agreement with Kapoor's results, and the x-ray yield per fragment would increase for the heaviest fragments possibly giving a striking increase for masses greater than 145. This last effect would be in agreement with our kinetic energy results.

IV. SUMMARY

The results for the three-parameter measurement of the prompt K x rays from thermal-neutron fission of U^{235} are presented. Except for the heaviest heavy fragments, the x-ray yields per fragment as a function of mass are in good agreement with both the results of Kapoor for thermal-neutron fission of U^{235} and the results of Glendenin for spontaneous fission of Cf^{252} . The results of Z_p versus mass are in agreement with radiochemical measurements.

The results for the x-ray yield per fragment as a function of mass for the heaviest heavy fragments are in agreement with Kapoor, and do not appear to show the striking increase shown by Cf^{252} . Our experiment looked at details made possible through a three-parameter analysis and could see relationships not possible with Kapoor's method. Because of the results found for these relationships, we cannot conclude that the apparent difference between Cf^{252} and U^{235} is real.

ACKNOWLEDGMENTS

The authors wish to express their gratitude to G. Beck, P. Hesselmann, and O. Whipple for their help and patience with the reactor operations, and to W. Sullivan for his help with the experiment.

²³ A. C. Wahl (private communication).